PERFORMANCE EVALUATION AND CALIBRATION OF THE NEURO-PET SCANNER

Victor J. Sank, Rodney A. Brooks, Walter S. Friauf, Stephen B. Leighton, Horace E. Cascio, and Giovanni Di Chiro
National Institutes of Health
Bethesda, Maryland 20205

Summary

The Neuro-PET is a circular ring seven-slice positron emission tomograph designed for imaging human heads and small animals. The scanner uses 512 bismuth germanate detectors 8.25 mm wide packed tightly together in four layers to achieve high spatial resolution (6-7 mm FWHM) without the use of beam blockers. Because of the small 38 cm ring diameter, the sensitivity is also very high: 70,000 c/s per true slice with medium energy threshold (375 keV) for a 20 cm diameter phantom containing 1 μCi/cc of positron-emitting activity, according to a preliminary measurement. There are three switch-selectable thresholds, and the sensitivity will be higher in the low threshold setting.

The Neuro-PET is calibrated with a round or elliptical phantom that approximates a patient's head; this method eliminates the effects of scatter and self-attenuation to first order. Further software corrections for these artifacts are made in the reconstruction program, which reduce the measured scatter to zero, as determined with a 5 cm cold spot. With a 1 cm cold spot, the apparent activity at the center of the cold spot is 18% of the surrounding activity, which is clearly a consequence of the limits of spatial resolution, rather than scatter. The Neuro-PET has been in clinical operation since June 1982, and approximately 30 patients have been scanned to date.

Description

The Neuro-PET scanner[1,2] began routine clinical operation in June of 1982; at the time of writing about 30 patients have been scanned. This 4-ring 7-slice positron emission tomograph was designed to fill the need for a high resolution, high sensitivity scanner at the National Institutes of Health for human head and animal studies. At the present time the electronics for three rings is operational, permitting simultaneous scanning of five slices; the remaining electronics chassis containing discriminators for the fourth ring will be installed shortly.

To achieve the mutually desirable goals of high resolution and high sensitivity, we designed each ring to contain 128 tightly packed bismuth germanate crystals 8.25x20x35 mm around a 38 cm circle (inside diameter). The reason for the small ring diameter is to increase the sensitivity, an extremely important consideration when doing high resolution scanning. In addition, we didn't want the number of detectors per ring to exceed 2^7.

The collimator assembly contains three washer-shaped disks of depleted uranium 3 mm thick, for reducing the number of scattered and out-of-plane detected gamma rays. This assembly reduces the patient aperture to 25 cm diameter, which so far has presented no difficulties in patient scanning, although the dental chair used for patient support has not been adequate for a few patients who could not sit up or lie in a supine position. One study done without the collimator has produced images of good quality, so that this modality may be used when a larger patient aperture is required.

Crystal face center-to-center spacing is 9.3 mm, so that a scanning motion is required to produce the sampling needed for maximum spatial resolution. Details of the wobble motion used have been reported previously.[3] This motion, which is under the control of a single SLOSYN stepper motor connected with a chain drive to two of the three eccentric shafts, is software controllable and has performed flawlessly to date. We currently use an 8 mm wobble diameter with 8 discrete data acquisition points spaced uniformly around the wobble circle.

The random coincidence count rate is a function of the coincidence resolving time τ of the electronic detectors, as well as of the single gamma count rate per detector. The Neuro-PET offers two switch-selectable resolving times, although all studies to date have been done with the longer τ of 12 ns. For dynamic studies with very high count rates the 5.5 ns τ may be used to further reduce the random coincidence rate, with a sensitivity reduction of 39%.

Performance Evaluation

Spatial resolution

Spatial resolution of the Neuro-PET was measured by scanning a line source placed in a 20 cm diameter solid plastic phantom. The source contains ^{68}Ge enclosed in a 3 mm diameter steel jacket to suppress the positron range; thus the results are fully representative of imaging with the isotope ^{18}F, which has a very small positron energy. All measurements were made on the reconstructed image without any software smoothing. This is the same reconstruction method used for patient images, although at the present time some patient images are later smoothed to reduce statistical noise due to limited counts. The need for this smoothing is expected to disappear when all seven slices are operational.

The full width at half maximum (FWHM) of the reconstructed line source image was found to be 6 mm at the center of the field of view, and 7 mm if the source is placed 9 cm off center. These values apply to both true and cross slices. In the near future we plan to increase the number of wobble points from 8 to 9, and to improve the method of interpolation from a linear approach to a multi-point polynomial approach. We believe that these improvements will enable us to achieve a resolution approaching 5 mm at the center of the field of view. In addition, we plan to provide optional beam blockers which will reduce the size of the detector apertures and thereby offer a resolution capability of 3-4 mm, although at the expense of reduced sensitivity. The beam blockers will be designed primarily for use with animal studies.

Sensitivity

Our sensitivity measurements were made using the conventional 20 cm diameter phantom containing a uniform distribution of activity. The phantom had a thin stainless steel wall to reduce the effect of wall attenuation, and the count rate was kept low enough that the effects of random coincidences and dead time were negligible. When the count rate was divided by the activity concentration, we obtained a sensitivity of 70,000 (c/s)/(μCi/cc) for a single true slice, using the medium energy threshold. This value is higher than we had anticipated, based on measurements reported with prototype components.[2] Part of the reason for the

discrepancy is that the earlier phantom had 1 cm thick plastic walls, and part may be due to the method of calibrating the activity. Until we investigate the matter further, the values reported herein must be regarded as tentative.

The sensitivity measured for a single cross-slice is 80,000 c/s, providing a total sensitivity for all seven slices of 520,000 (c/s)/(μCi/cc) at medium threshold. The sensitivity at low and high energy thresholds has not yet been determined, but our present feeling based on patient studies done to date is that the improvement in sensitivity offered by the low energy threshold will be of significant help in reducing statistical noise, and that this modality with its increased sensitivity may become more widely used.

Scatter

The effect of scattered coincidences was evaluated using cylindrical "cold spots" placed in a 20 cm diameter phantom filled with a uniform distribution of activity. One cold spot was a 5 cm diameter plastic tube filled with water; the other was a 1 cm diameter plastic rod. After scanning the phantom, the image was reconstructed the same way as patient images, and the apparent activity in the center of the cold spot was measured. The 5 cm cold spot was scanned in the center of the phantom, and the 1 cm cold spot was scanned approximately 7 cm from the center.

The results showed an apparent activity of zero for the 5 cm cold spot, not only at the center of the spot, but throughout the entire area. For the 1 cm cold spot the apparent activity at the center was 18% of the surrounding activity. This 18% figure obviously is due to the tails of the line spread function, rather than to scatter, since the 5 mm radius of the rod is less than the FWHM of the line spread function. These results show that the scatter correction program in the reconstruction routine is operating properly.

To evaluate the scatter without software correction, reconstructions were made in which the correction was omitted. In this case the apparent activities were 19% for the 5 cm cold spot and 33% for the 1 cm cold spot. We therefore conclude that, at the medium energy threshold, the scatter contribution in the Neuro-PET scanner is 15-20% before software correction and zero afterward. However, we must emphasize that the present scatter correction program is not very sophisticated and will not perform as well when the distribution of activity is more complicated than a single cold spot. A more accurate program is under development.

Patient images

Approximately thirty patients have been scanned to date with ^{18}F-deoxyglucose (FDG), a radiopharmaceutical which is taken up in proportion to the glucose utilization rate of the tissue. These images thus provide a metabolic map of the brain. The Neuro-PET has produced images with excellent delineation of the cerebral cortex and separation of the basal ganglia, and has proven particularly invaluable in revealing the very thin rim of malignant tissue that sometimes is found in gliomas that possess a large necrotic center.

Figs. 1-5 illustrate typical results obtained for both normal and pathological structures. Because of limited counts, these pictures have been smoothed slightly, using the SMOOTH option of the VIEW program. The resultant spatial resolution has thus been degraded approximately 1 mm beyond the values quoted earlier. We expect that the need for smoothing will disappear when all seven slices are operational, so that longer scans can be made. The scan time for most of these studies was 10 minutes. We should also mention that quantitative measurements made with the Region of Interest program are based on unsmoothed image numbers, and so are not degraded by the smoothing which is done solely for visual appearance.

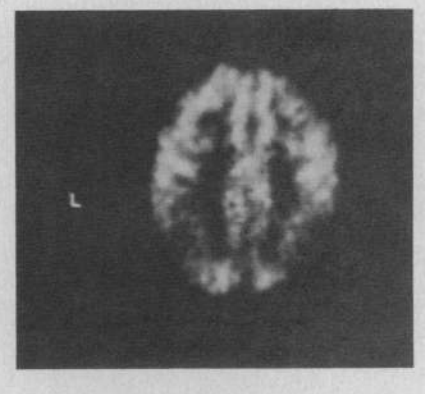

Fig. 1. Tomogram through the convexity of the brain showing good delineation of the peripheral and midline cerebral cortex. Note in particular the interhemispheric fissure and the clear separation between white matter (dark areas) and gray matter (bright).

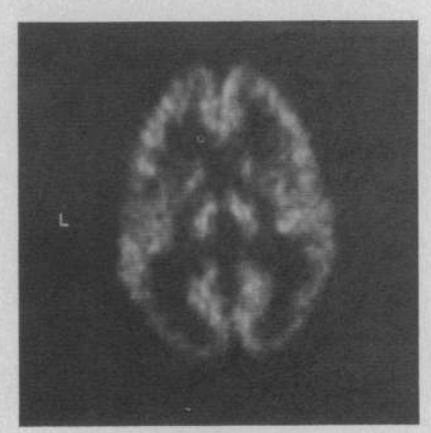

Fig. 2. Tomogram at the level of the basal ganglia. Note also the separation of the right and left posterior cortex.

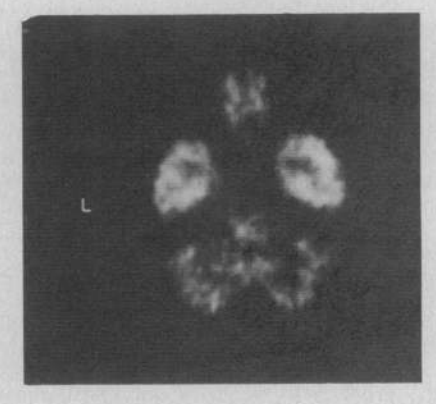

Fig. 3. Scan showing the temporal lobes and the cerebellum. Note the distinction between white matter + temporal horns (darker areas) and cortex in the depth of the temporal lobes.

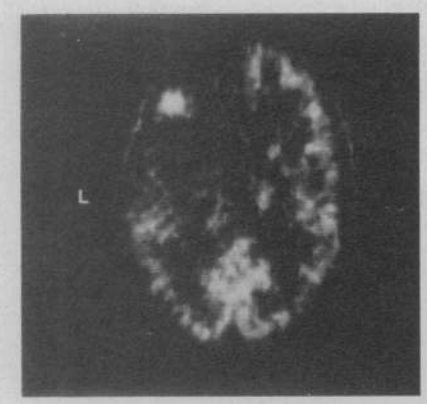

Fig. 4. Malignant glioma (bright spot) in the anterior left hemisphere. The reduced intensity in the greater part of this hemisphere is due to edema associated with the tumor.

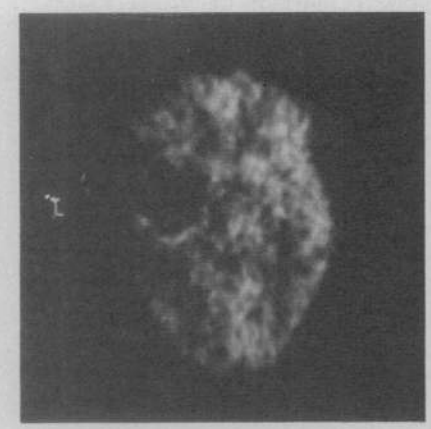

Fig. 5. A glioma in the left hemisphere exhibiting a large necrotic center (dark area) outlined posteriorly by a thin bright rim of viable tumoral tissue.

CALIBRATION

The Neuro-PET detectors are calibrated in a unique manner, as compared with other PET scanners. Most other scanners use an annular phantom, or a sheet phantom, in order to apply a known amount of radioactivity between each pair of detectors.[4,5] Subsequent software corrections are then made during the reconstruction of patient scans for scatter, self-attenuation, and random coincidences.

The approach used with the Neuro-PET is similar to that used in some CAT scanners, in that a cylindrical or elliptical phantom approximating the shape of a patient's head is used for calibration. CAT scanners have a problem with beam-hardening artifact which is analogous to self-attenuation in PET in that both, if uncorrected, produce a "cupping" artifact wherein the intensity at the center of the image is reduced in intensity. In addition, scattered photons are a problem with both modalities, adding a background haze to the image. Several CAT manufacturers have found that by calibrating the detectors with a round phantom of suitable diameter, these problems can be eliminated to first order. Software corrections can then be made for the residual error, which arises from the deviations between the actual patient geometry and that of the calibration phantom.

Up to the present time we have been using a 20 cm diameter cylindrical phantom, although the software programs allow for an elliptical phantom as well. The calibration procedure is as follows: The phantom is placed in the gantry and centered with respect to the detector ring, which is held stationary (no wobble) during the calibration scan. A typical calibration may last 30 minutes or more, to insure that the statistical inaccuracy in the calibration coefficients is substantially less than statistical fluctuations in patient scan data. Coincidence counts acquired during the calibration are stored in extended memory of the Data General Eclipse S/250 computer, using the same data acquisition system as for patient scanning. The calibration program then performs the following calculations for each detector pair (see also Fig. 6):

Random coincidences. Random coincidences cannot be included in the calibration coefficients, as is done for scattered coincidences, because the random rate is proportional to the square of the true count rate. The total random coincidences for each detector pair are calculated from the single count rates of the individual detectors and subtracted from the accumulated counts.

Decay correction. The number of counts is decay corrected to the time at which the activity concentration was measured. This decay correction takes into account the exponential nature of the decrease during the calibration scan. This is important because ^{68}Ga, with a half-life of only 69 minutes, is often used for calibration.

Path integral. The activity concentration (nCi/cc) is measured in a well counter and entered into the computer. The computer then calculates the path length through the phantom of the ray connecting the two detectors, using the proper geometrical formula for an ellipse. The product of the activity concentration and the path length gives the ideal path integral (nCi/cm^2) for that ray.

Calibration coefficient. The ratio of the corrected counts per second to the ideal path integral is then calculated and stored in a disk file called CAL.

The above calculation is done for 28,672 detector pairs (7 slices x 128 views per slice x 32 detector pairs per view). The cross slice coefficients actually contain contributions from two detector pairs, e.g., 1A-64B and 1B-64A, where A and B refer to two adjacent rings; however the calibration coefficient is calculated for the combined count rate, not for the individual pairs. In addition, the Neuro-PET offers 3 switch-selectable energy thresholds and 2 coincidence resolving times, making a total of six possible combinations, and calibration coefficients must be obtained for each setting. All of our present patient scans have been done with medium threshold and the long coincidence resolving time.

The advantage of this method of calibration is that the coefficients automatically include the effects of scatter and self-attenuation for a uniform distribution of activity, as well as the geometrical and physical sensitivity factors for each detector. Our philosophy is to include as much as possible into the calibration so that the amount of correction that must be

```
      ACCEPT "Enter activity concentration (nCi/cc): ", CONC
      ACCEPT "Enter time of measurement (H,M,S on computer clock): ",TMEAS
      T = 60*(TSTART(1)-TMEAS(1))+TSTART(2)-TMEAS(2)+(TSTART(3)-TMEAS(3))/60
      C1 = CONC*EXP(-LAMBDA*T)*60*(1-EXP(-LAMBDA*TSCAN))/LAMBDA
      IF (LAMBDA.LT.1E-5) C1 = CONC*60*TSCAN
      T = 60*(TSTART(1)-TSING(1))+TSTART(2)-TSING(2) + (TSTART(3)-TSING(3))/60
      C2 = TAU*EXP(-2*LAMBDA*T)*60*(1-EXP(-2*LAMBDA*TSCAN))/LAMBDA
      IF (LAMBDA.LT.1E-5) C2 = 120*TAU*TSCAN*EXP(-2*LAMBDA*T)
      DO 41 IS=1,2*NRING-1                                    7 slices
      IBLOCK = (3-ITAU)*672+(ITHRESH-1)*224+(IS-1)*32  ;Starting block of CAL
      IR = (IS+1)/2
      ICROSS = MOD(IS+1,2)      ;ICROSS = 1 for cross-slice, 0 for true slice
      A0 = 16
      B0 = 113
      COUNTS = 0.
      DO 40 JPAGE = 1,4;  Go to one page of data at a time
        CALL REMAP(MAP(32*IB+JPAGE-1+4*IS),0,1,IER)
      DO 40 J1=1,32; Process 32 views per page                128 views
        J = J1 + (JPAGE-1)*32
        M = 2-MOD(J,2); M=1 for odd view (with central ray), 2 for even view
        PHI = PI*(J-1)/128
        RHO2 = (URAD*SIN(PHI))**2 + (HRAD*COS(PHI))**2 ;Square of eff. radius
        C3 = 2*C1*URAD*HRAD/RHO2       ;Used in CAL formula
        DO 30 ID=1,32                                         32 detector pairs
          ARG = RHO2 - DP(ID,M)**2
          IF(ARG.LE.0) CAL(ID,J) = 0              ;if outside phantom, CAL = 0
          IF(ARG.LE.0) GO TO 30                   ;and skip calculation
          A = A0 + ID             ;A and B are detector numbers for ray (ID,J)
          B = MOD(80-ID,128) + 1
          IF(ICROSS.EQ.0) RAND = C2*C(A,IR)*C(B,IR)     ;Random correction
          IF(ICROSS.EQ.1) RAND = C2*(C(A,IR)*C(B,IR+1)+C(B,IR)*C(A,IR+1))

        CAL(ID,J) = C3*SQRT(ARG)/(WINDOW(ID,J1)-RAND)   ;THIS IS CAL FORMULA!

        COUNTS = COUNTS + WINDOW(ID,J1)
        IF(WINDOW(ID,J1).LT.10) CAL(ID,J) = 1E6 ;Flag bad CAL if counts are low
30      CONTINUE
      IF (M.EQ.1) A0 = A0 + 1
40    IF (M.EQ.2) B0 = B0 + 1
```

Fig. 6 Portion of calibration program in which coefficients CAL(ID,J) are calculated for the IDth detector pair in the Jth view. The raw counts are stored in four pages of extended memory and accessed through an array WINDOW(ID,J1), where ID is the number of the detector pair and J1 is the view number within the page.

applied later during reconstruction is held to a minimum. By including first-order scatter and attenuation in the calibration coefficients, we do not ignore these problems -- we take them into account in the simplest most direct manner.

Peripheral calibration

The disadvantage of the above calibration method is that it applies only to those detector pairs which transect the phantom. If the phantom is at least as big as the largest patient head, this is not a problem, as long as the patient is properly centered. However it is clearly desirable to have a proper calibration for the entire 25 cm aperture, i.e., for all 32 detector pairs per view. At the time of writing, this has not been accomplished, but we have the following approaches in mind for extending the calibration. One idea is to use a separate annular phantom, as others have done. Another idea is to use the scatter skirts of the round phantom for calibrating the peripheral detectors. In either case, the problem will be to develop a smooth transition between the two areas of calibration, since the inner detector pairs include the scatter in the coefficients, and the outer ones will not.

References

1. RA Brooks, VJ Sank, G Di Chiro, WS Friauf, SB Leighton, "Design of a high resolution positron emission tomograph: The Neuro-PET". J Comput Assist Tomog 4, 5-13 (1980)

2. RA Brooks, VJ Sank, WS Friauf, SB Leighton, HE Cascio, G DI Chiro, "Design considerations for positron emission tomography". IEEE Trans Biomed Eng BME-28, 158-177 (1981)

3. RA Brooks, VJ Sank, AJ Talbert, G Di Chiro, "Sampling requirements and detector motion for positron emission tomography". IEEE Trans Nucl Sci NS-26 (1979)

4. M Bergstrom, L Eriksson, C Bohm, G Blomqvist, "A procedure for calibrating and correcting data to achieve accurate quantitative values in positron emission tomography". IEEE Trans Nucl Sci NS-29, 555-557 (1982)

5. DC Ficke, DE Beecher, GR Hoffman, JT Hood, J Markham, N Mullani, MM Ter-Pogossian, "Engineering aspects of PETT VI". IEEE Trans Nucl Sci NS-29, 474-478 (1982)